9-2019

Structures, properties, and applications of CNT-graphene heterostructures

Wei Du

Zubair Ahmed

Qi Wang

Cui Yu

Zhihong Feng

See next page for additional authors

Recommended Citation

Du, W., Ahmed, Z., Wang, Q., Yu, C., Feng, Z., Li, G., Zhang, M., Zhou, C., Senegor, R., & Yang, C. Y. (2019). Structures, properties, and applications of CNT-graphene heterostructures. 2D Materials, 6(4), 042005. https://doi.org/10.1088/2053-1583/ab41d3

Structures, Properties, and Applications of CNT-Graphene Heterostructures

Wei Du[1], Zubair Ahmed[2], Qi Wang[1], Cui Yu[3], Zhihong Feng[3*], Guoyuan Li[1], Min Zhang[4], Changjian Zhou[1*], Richard Senegor[5], and Cary Y. Yang[5]

[1]School of Microelectronics, South China University of Technology, Guangzhou 510641, China

[2]Department of Electronic and Computer Engineering, The Hong Kong University of Science and Technology, Kowloon, Hong Kong, China

[3]National Key Laboratory of ASIC, Hebei Semiconductor Research Institute, Shijiazhuang 050051, PR China

[4]School of Electronic and Computer Engineering, Peking University, Shenzhen 518055, China

[5]Center for Nanostructures, Santa Clara University, Santa Clara, California, USA

*Corresponding Author：ga917vv@163.com and zhoucj@scut.edu.cn

Abstract：Both carbon nanotube (CNT) and graphene exhibit excellent properties and have many potential applications in integrated circuits, composite materials, thermal management, sensors, energy storage, and flexible electronics. However, their superior properties are confined to one or two dimensions, thus limiting their utility in interconnects or thermal interface materials that require a three-dimensional structure for efficient electron and/or phonon transport. It is conceivable that a combined CNT-graphene structure would provide new opportunities for realizable applications in these and other fields. In recent years, numerous results on synthesis, structural analyses, theoretical modeling, and potential applications of various CNT-graphene heterostructures have been reported. In this review, we summarize the possible structures that can be formed by connecting CNT and graphene. We then report existing experimental efforts to synthesize the heterostructures based on growth method, catalyst design, and the resulting properties. Also, theoretical studies on various heterostructures are reviewed, with the focus on electron and thermal transport within the heterostructure and across the CNT-graphene interface. Several potential applications are briefly discussed, and a combined theoretical and experimental approach is proposed with the objective of enhancing the understanding of the CNT-graphene heterostructure and attaining a realistic assessment of its feasibility in practical applications.

1. Introduction

Since the discovery of fullerenes[1], the family of nanocarbon allotropes has been studied extensively due to the carbon-carbon bond versatility [2, 3], with carbon nanotube (CNT) and graphene being the most well-known[4, 5]. The superior properties of these nanocarbon materials such as their large surface-to-volume ratios, electrical and thermal transport, tunability of band structure by applied voltage [6-8], magnetic field [9, 10], and mechanical strain[11-13], as well as synthesis methods have paved the way for practical applications in nanoelectronics, electrochemistry, sensors, and supercapacitors[14-17]. However, such properties have not been fully exploited in many potential applications. This is partly due to the non-uniformity of the synthesized nanocarbon [18, 19], resulting from the non-ideal interface between the nanocarbon and other constituent materials [20-26]. For example, CNT has long been considered as a promising material to replace copper in on-chip interconnects as the current density in copper lines exceeds its current-carrying capacity [27-30]. In reality, although researchers have demonstrated CNT vias down to sub-100 nm dimensions [31-33], the resistance of the CNT vias is still much larger than that of mainstream copper interconnects. Such large interconnect resistance is mainly due to contact resistance between the CNTs and other conductors [21, 22, 24, 34]. Many efforts have been devoted to reducing the contact resistance for carbon-based electron devices [35]. Since both graphene and CNT have the same honeycomb structure, a seamless contact between them appears possible[36]. A three-dimensional all-carbon structure consisting of CNT-on-graphene could realize excellent electrical and thermal conduction in both horizontal and vertical directions. Such a structure could then serve as a building block in on-chip interconnects.

In applications that aim to take advantage of the large surface-to-volume ratio

in CNT and graphene, such as electrodes in supercapacitors, batteries, and reactive catalysts [37-39], it is challenging to prevent the aggregation of the nanocarbons [40, 41]. In contrast, if a heterostructure consisting of vertical CNT arrays and horizontal graphene layers is formed, a more robust structure is expected to resist the aggregation tendency while still preserving the high surface-to-volume ratio [42, 43], electrical and thermal transport[44, 45], optical and optoelectronic properties[46], and tunability of band structure by applied voltage[6-8] and magnetic field[9, 10, 47].

With the objective to fully exploit the extraordinary properties of nanocarbons, researchers in various disciplines, including electronics [48, 49], material science [50], mechanical engineering [51], and chemistry[52], have explored the possibility of combining these two most well-known nanocarbon allotropes during the last decade. Therefore, it is meaningful to review what has been achieved, and what can be expected in future studies of the CNT-graphene heterostructure.

This paper is organized as follows. The next section describes the basic structures of and synthesis methods for CNT-graphene heterostructures, followed by a review of theoretical studies based on techniques including first-principle calculations and molecular dynamics simulations. We then present various potential applications of the heterostructures. Finally, we conclude with a discussion of what is needed to fully optimize the heterostructure for practical applications.

2. Structures and Growth Methods

2.1 Structures

To make full use of the structure and properties of the 1D CNT and 2D graphene , various methods have been proposed to prepare CNT arrays[53], while graphene, with its two-dimensional planar structure, is usually grown on metal foils or thin films[54]. Although both show promise in many applications, it is beneficial to

combine them into a single CNT-graphene heterostructure, which not only preserves the excellent properties of the two materials, but also compensates for each other's shortcomings to some extent. Generally, CNT grows along the axial direction, thus forming CNT arrays vertical or parallel to the substrate. Several possible models of joining CNTs and graphene are illustrated in Figure 1. A parallel CNT-graphene heterostructure[55-58] (Figure 1a) can be obtained by drop-casting CNT on the transferred graphene, or graphene can be transferred to cover the CNT network to form a similar structure but with graphene on top[59]. While these two structures preserve the two-dimensional structure as in graphene, it is desirable to form a truly three-dimensional structure by joining vertical CNTs and planar graphene. Figure 1b shows a typical structure with the CNT axis normal to the graphene plane [42, 60-65], forming a vertical CNT-graphene heterostructure. In certain cases, the graphene can be lifted off during the CNT growth, thus forming a structure as shown in Figure 1c [66-69]. Recently, several experimental works claimed to obtain seamless CNT-graphene heterostructures[36, 70] (Figures 1d and 1e). Multilayered vertical CNT-graphene heterostructure was also reported as an all-carbon pillared structure [71] (Figure 1f), in which graphene was used as the platform for CNT growth and the grown CNTs served as pillars to support graphene layers. In principle, the seamless junctions between CNT and graphene can yield a more robust mechanical structure with enhanced interplanar electrical and thermal conduction.

In general, compared to the parallel CNT-graphene heterostructure, the vertical CNT-graphene configuration is more desirable for applications that require low electrical resistance. Gao[72] compared the resistance of the parallel and vertical CNT-graphene heterostructures, Gao [72] compared the resistances of the parallel and vertical CNT-graphene heterostructures, and found that the parallel heterostructure exhibited a contact resistance of 51.9 kΩ, which is nearly four times the contact resistance of 14 kΩ in the vertical heterostructure. The difference is

likely due to the unsaturated π-bonds of edge atoms in the vertical CNT configuration, giving rise to stronger bonding with atoms in the graphene layer. Based on the development of the different pillared heterostructures, theoretical and experimental analyses of the CNT-graphene-CNT heterostructure (Figure 1f) have been carried out in recent years[71, 73-77].

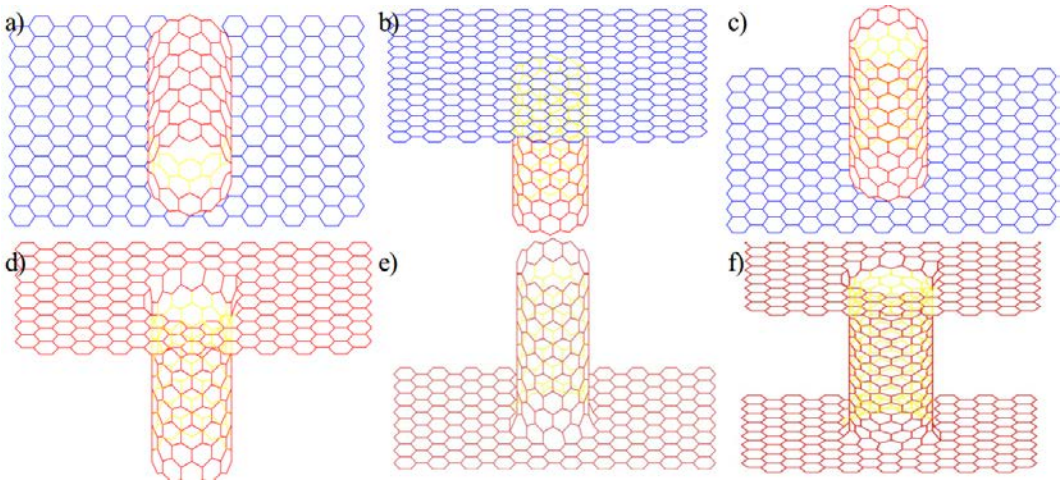

Figure 1. Schematic illustrations of the (a) parallel CNT-graphene heterostructure, (b, c) normal CNT-graphene heterostructure, (d, e) seamless CNT-graphene heterostructure, and (f) CNT-graphene-CNT heterostructure.

2.2 Growth methods

As there are many excellent reviews on the growth of CNT and graphene [53, 78-80], the focus of this paper is on the growth of the heterostructure itself. Specifically, we discuss the various parameters for growth of CNT-graphene heterostructures, including the overall methodology, catalyst requirement, growth temperature, and properties of the resulting structure.

2.2.1 Parallel CNT-graphene heterostructures

Parallel CNT-graphene heterostructures are generally formed using chemical vapor deposition (CVD) [57, 81, 82]. In such a method, a graphene film is synthesized first, followed by catalyst deposition on the graphene and then CNT growth to form the parallel CNT-graphene heterostructure. For example, using $FeCl_3$ solution deposited on graphene as catalyst, CNTs were formed on the dried sample after the introduction of argon/hydrogen/acetylene (30/30/5sccm) at 750°C[81]. It was

determined that the density and the quality of the CNTs was related to the concentration of the $FeCl_3$ solution. The density of CNTs can be well controlled simply by choosing the corresponding concentration for a targeted density requirement. On the other hand, the use of the $FeCl_3$ is avoided in many cases because of the potentially hazardous waste it creates. With CNTs as the template, a CNT spider web was firstly deposited on a copper substrate[82], then a xylene solution consisting of ferrocene and sulfur was injected into CNT webs, followed by high-temperature annealing. The parallel CNT-graphene heterostructure was then formed with the introduction of a carbon source, and the CNTs served as nucleation centers during the graphene growth, as shown in Figure 2a. This cage-growth method ensures good matching between CNT network-embroidered graphene film and graphene, which contributes to the development of all-carbon devices.

An alternative method used graphene as the growth template, on which the CNTs were directly deposited without carbon source gas [57]. It was found that CNTs in the parallel heterostructure lay mainly along the armchair axes of the graphene film (Figure 2b). To obtain better aligned CNT-graphene heterostructure, coating the CNTs on graphene was used, while ensuring that the CNTs and graphene were firmly connected. Figure 2c shows the graphene film coated with cross-folded CNT networks[83]. After etching the Cu substrate, a self-standing parallel CNT-graphene heterostructure was obtained. The CNT-graphene film obtained by the facile method has ~90% electron transparency, which is suitable for high-performance electrode applications.

Various methods have been proposed to increase the CNT density and thus the electrical performance of the resultant heterostructure. Wu[55] adopted a blown bubble method to prepare the aligned CNT arrays on top of graphene (Figure 2d). Multiwall CNTs (MWCNTs) were grown first, and a CNT solution with PMMA and acetone as the solvent was prepared to form the bubble solution. Aligned CNTs were obtained due to surface tension of the bubble. The CNT density was increased

by simply repeating the bubble transferring process. The final high-temperature annealing process could enhance the bonding between CNT and graphene, which is beneficial for electrical and thermal applications.

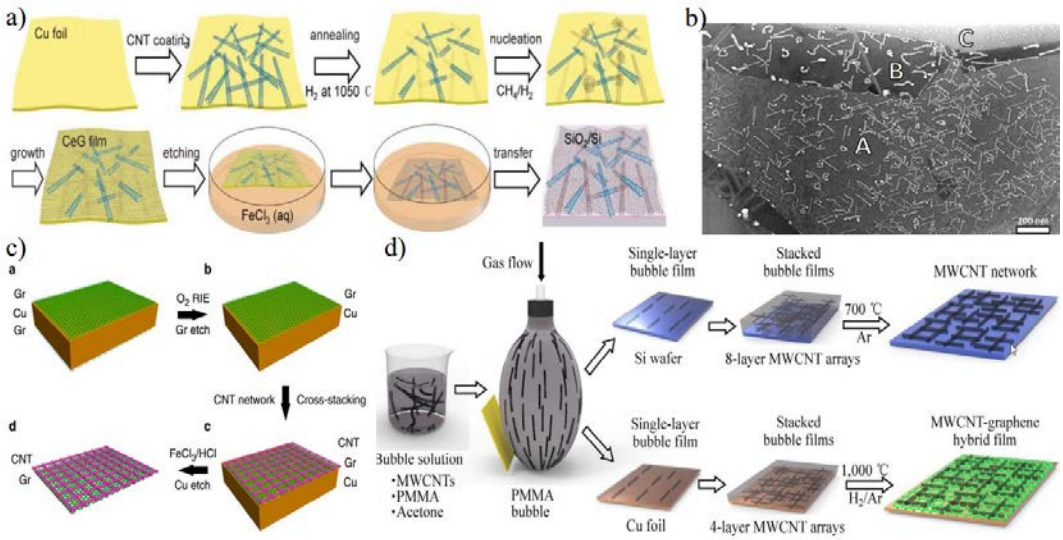

Figure 2. Scheme for CNT-graphene parallel heterostructure. (a) Graphene grown by Chemical Vapor deposition using CNTs as templates [82]. (b) CNTs grown by Chemical Vapor deposition using graphene film as template [57]. (c) Cross-staking CNT networks coated on the graphene film[83]. (d) By blown bubble method[55].

2.2.2 Vertical CNT-graphene heterostructure

In general, CVD[50, 83-90] is the most common method for synthesizing vertical CNT-graphene heterostructures, using a two-step process as illustrated in Figure 3 [91]. First, graphene is grown on a metal substrate and subsequently transferred onto a target substrate if needed. Second, the vertical CNT-graphene heterostructure is synthesized after catalyst deposition and introduction of a carbon source gas. There are many factors that affect the growth, and we will focus on the effects of catalysts, temperature, and gases on the characteristics of the resulting heterostructure.

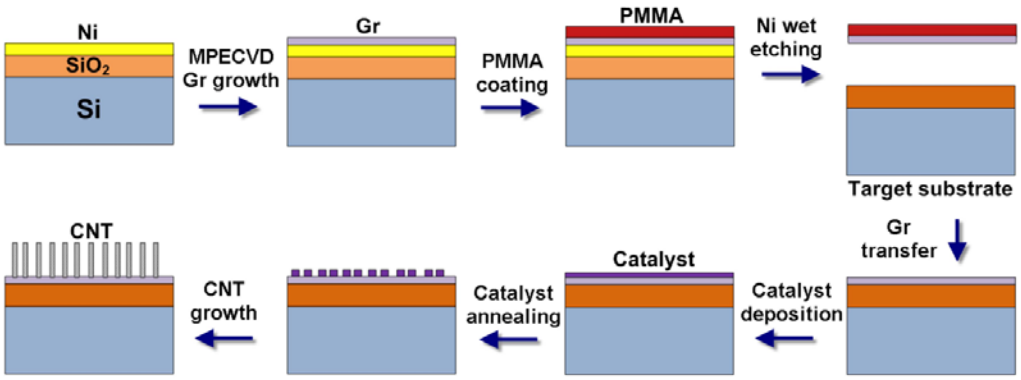

Figure 3. A two-step process for CNT-graphene heterostructure preparation[91].

Experiments on the choice of catalyst using different thicknesses of Fe or Ni have been carried out[91]. It was found that if the Fe film thickness could be controlled within a range of 0.2 nm to 1 nm, better quality of CNTs was obtained for thinner films, as confirmed by Raman analyses. When the Fe film thickness was as low as 0.5 nm, single-walled CNTs (SWCNTs) were obtained. Otherwise, MWCNTs resulted whether Fe or Ni was used as the catalyst[91]. The diameter of the CNTs is largely affected by the catalyst film thickness. In addition, the effects of Ni and Fe catalyst on formation of the CNT-heterostructure are quite different, as Ni etches graphene during the growth process, leading to more defects in the final structure. It is worth noting that the etching of the graphene is expected, because in the early stages of CNT growth, graphene is a carbon source in addition to the carbon source gas. And H_2 also plays an important role in the etching of graphene because of the reaction [63]

$$(Ni)_{nanoparticle} + C_{graphene} + 2H_2 \rightarrow Ni + CH_4$$

The growth temperature and gas feedstock can be tuned to minimize graphene etching. By using C_2H_4 as the carbon source, the Ni catalyst film can form higher density nanoparticles at 700°C and the etching becomes less reactive compared to 800°C, resulting in higher density CNTs and less etching of graphene[63].

Apart from graphene etching, catalytic nanoparticles become embedded in the CNT-graphene junctions in some cases, which limits the properties of the

heterostructure. To prevent this effect and form a seamless CNT-graphene heterostructure, Zhu[36] deposited a layer of Al_2O_3 film on the Fe catalyst film as a floating buffer layer (Figure 4a). The floating buffer was designed to transform the bottom growth of the CNTs into tip growth, thus achieving the goal of a seamless CNT-graphene heterostructure with optimal interface properties. Similarly, the heterostructure was successfully[89] synthesized on a porous Ni foam by using the same method but with a better area utilization ratio of the metal substrate, as shown in Figure 4b. Inspired by this method, Jiang[77] realized that CNTs could grow from both sides of graphene, as shown in Figure 4c. This unique structure has the potential to be used in energy storage that requires a high surface-to-volume ratio.

Instead of using solid catalyst films, Rodrigo[70] spun a solution of Fe_3O_4/AlO_x nanoparticles as the catalyst on the graphene/Cu substrate, which is also applicable to curved substrates. Being exposed to hydrogen at 750℃, the catalyst nanoparticles became a mixture of Fe and Al_2O_3. Then a seamless CNT-graphene heterostructure was formed via tip growth mechanism, with the covalent C-C bonds at the CNT-graphene junction, as shown in Figure 4d. By using Fe catalyst, SWCNTs can be grown at 950℃ on a FeMgAl layered double oxide substrate[92], with the process shown in Figure 4e. Compared to MWCNT, SWCNT arrays have a higher surface-to-volume ratio and smaller defect density, while forming covalent C-C bond at the CNT-graphene interface, leading to better electron transport[92]. The superior properties of the SWCNT-graphene heterostructure are suitable for applications as electrodes in high energy density batteries.

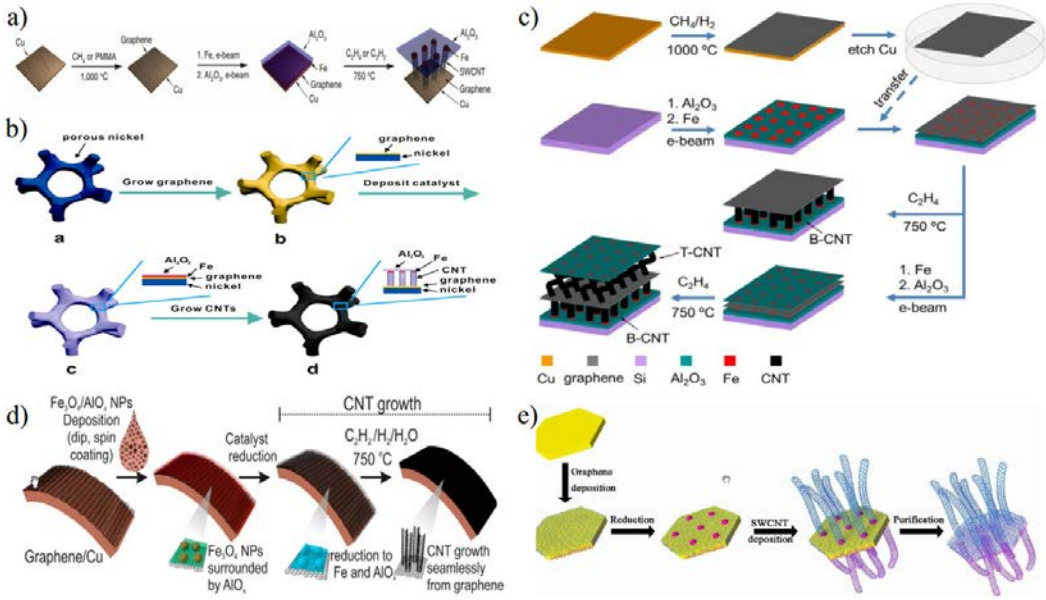

Figure 4. Scheme for CNT-graphene vertical heterostructure. (a) synthesis of CNT carpets directly from graphene by adding a layer of Al_2O_3 film on Cu substrate[36]. (b) synthesis of seamless CNT-graphene heterostructure by adding a layer of Al_2O_3 film on porous Ni substrate[89]. (c) CNTs grown from both sides of graphene using supporting layer: Al_2O_3 films[77]. (d) Using solution of Fe_3O_4/AlO_x nanoparticles as catalyst[70]. (e) Growing seamless SWCNT-graphene heterostructure on FeMgAl layered double oxide substrate[92].

In general, all catalyst film thicknesses in the two-step method are between 1 and 10 nm or thinner to yield good-quality CNTs. With increase in catalyst film thickness, graphene can also be formed. Therefore, CNT and graphene can be grown simultaneously if the thickness of the catalyst can be controlled within a few nanometers. Instead of the two-step growth method, a one-step method is also feasible for forming vertical CNT-graphene heterostructures, thus simplifying the growth process. Kondo[67] deposited different thickness of Co film on 5 nm TiN to form a mixed catalyst. The thickness of the Co catalyst is within a few nanometers so that both graphene and CNTs can be synthesized using Co catalyst. With the gas ratio of acetylene to argon being 1:9, graphene films were formed first, then the Co catalyst film dewetted to form nanoparticles, followed by CNT growth at 510℃

using tip-growth mode and resulting in a vertical CNT-graphene heterostructure on a silica substrate (Figure 5a). It was found that increased Co thickness resulted in increased graphene thickness.

Ni/TiN was also reported as a catalyst to synthesize CNTs and graphene[68]. Without conventional argon pretreatment, Jousseaume[68] used C_3H_6 as the carbon source gas rather than traditional C_2H_2 or CH_4, and prepared a vertical CNT-graphene heterostructure at 400°C using bottom-growth mode. The lower temperature ensures compatibility with chip manufacturing processes for the vertical CNT-graphene heterostructure to serve as part of an on-chip interconnect network. Furthermore, using FeMoMgAl layered double hydroxides as catalyst, a nitrogen-doped CNT-graphene heterostructure has also been achieved by the one-step method[93]. The schematic of the growth process is shown in Figure 5b. The specific surface area of the structure reached 812.9 $m^2\ g^{-1}$ and the electrical conductivity was as high as 53.8 S cm^{-1}. In addition, the structure had excellent bifunctional oxygen electrode activity for both oxygen reduction reaction and oxygen evolution reaction, which offers possibility to be a bifunctional electrocatalyst in metal-free devices.

Seamless heterostructures can also be obtained by the one-step method[94]. A typical example is shown in Figure 5c. First, an aluminum wire was exposed to 0.3M oxalic acid solution at 40 V and 3°C so that the external surface could be turned into anodized aluminum oxide. Then without catalyst, CNTs were seamlessly surrounded by a cylindrical graphene layer using CVD. In general, the key in the one-step growth is the proper choice of catalyst (material and thickness) and temperature to form the two constituent nanocarbon materials sequentially or simultaneously.

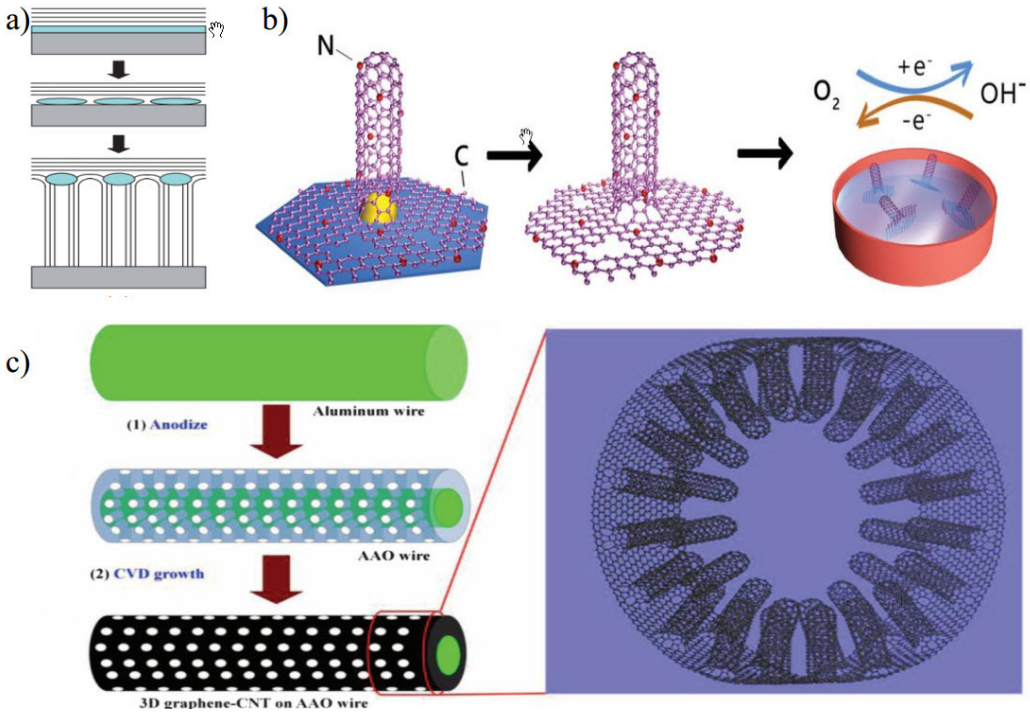

Figure 5. (a) Scheme of one-step method process[68]. (b) Process of the nitrogen-doped graphene/carbon nanotube hybrids growth[93]. (c) Schematic of radially aligned CNTs growth process[94].

It is expected that the seamless heterostructure shown in Figure 2(d)-(e) can provide superior electronic and thermal transport properties through the CNT-graphene junction as well as improved mechanical stability. However, there is still little evidence that the fabricated vertical structure possesses a seamless connection. Several proposed connection topologies between CNT and graphene are presented in the next section along with first-principle calculations. However, high-resolution transmission electron microscopy is needed to show experimentally how the carbon atoms are connected at the CNT-graphene junction. We hope that with more advanced characterization techniques, the atomic arrangement at the junction can be identified, and provide an experimentally confirmed structure for theoretical calculations.

3. Theoretical Studies of CNT-Graphene Heterostructures

Both CNT and graphene have extraordinary electronic transport properties, mechanical strength, and thermal conductivity. Until now, various theoretical methods have been employed to study the properties of CNT-graphene heterostructure, specifically to simulate seamless CNT-graphene heterostructures. In principle, there can be numerous geometrical configurations for both parallel and vertical CNT-graphene heterostructures, considering the various CNT chiralities, the number of walls in a CNT, the bonding type between CNT and graphene that could be van der Waals or covalent. Thus, it would not be practical to list all the possibilities of CNT-graphene heterostructures. Those that have been studied are constrained partly by the computational resources and the difficulty in establishing a stable junction between a CNT and graphene. Nevertheless, there are interesting properties revealed by various theoretical studies, though most remain unverified by experiment.

3.1 Parallel CNT-graphene heterostructure

As the parallel CNT-graphene heterostructure is mainly used for electrodes or all-carbon transistors, most theoretical studies have focused on its electronic properties[95-97]. Ho[95] studied the electronic structures of a non-chiral (armchair or zigzag type) CNT positioned flat on the underlying graphene, as shown in Figure 6a. The exact position of CNT is optimized using the Lennard-Jones interatomic potential, and the interlayer distance between CNT and graphene is around 3.1Å~3.2Å, implying that the bonding is van der Waals type. Compared to pristine CNT and graphene, the band structure of the heterostructure exhibits typical coupling effects between CNT and graphene, resulting in extra band-edge states at the intersecting linear bands, as shown in Figure 6b. The coupling effect can be further modulated by rotating the CNT relative to the in-registry position, but it generally weakens as the CNT diameter and the interfacial distance increases. One interesting phenomenon is the induced non-zero bandgap for pristine metallic (3m,

0) CNT due to coupling to the graphene, suggesting that even metallic CNT can be used for transistors if the CNT diameter is small and graphene is used as an underlying substrate. Similarly, Cook[96] calculated the charge redistribution between graphene and semiconducting (8,0) and (10,0) CNTs, and reported a very low Schottky barrier height between CNT and graphene. This is qualitatively verified by experimental results of Chai[98, 99], who applied graphitic interfacial contact layer to improve the CNT transistor properties, and of Ganggavarapu[98, 99], who achieved ohmic contact between CNT and few-layer graphene.

A seamless parallel CNT-graphene heterostructure with a (12,0) CNT covalently bonded to one or more graphene nanoribbons with the same width as the CNT length has been proposed[100-102]. A common feature of these structures is the sp^3-like bonding at the interface between CNT and graphene. Artyukh[102] studied the structure where the atoms at the edge of the two graphene nanoribbons are directly connected to the CNT wall, as shown in Figure 6c. Compared to pristine CNT or graphene, the density of states (DOS) of the heterostructure exhibits some similar Van Hove peaks, and resemble those in hydrogenated CNT, as shown in Figure 6d. In terms of mechanical strength, the heterostructure exhibits much higher Young's modulus due to the sp^3 bonds present at the interface[102].

3.2 Vertical CNT-graphene heterostructure

Vertical CNT-graphene heterostructures have potential applications in many fields such as electrodes, interconnects, transistors, catalyst, and thermal interface materials. Thus, the electronic and thermal transport properties are of much interest for these applications. In this sub-section, we focus mainly on the properties of modeled seamless vertical CNT-graphene heterostructures to examine its electronic and thermal transport properties.

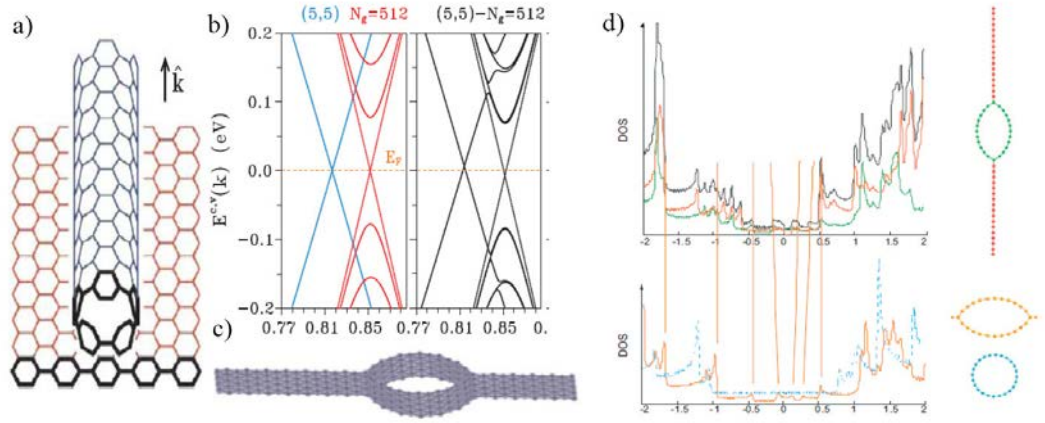

Figure 6. (a) Parallel CNT-graphene heterostructure with Van der Waals bond between CNT and graphene[95]. (b) Band structures of the CNT, graphene, and coupled CNT-graphene heterostructure[95]. (c) Parallel CNT-graphene heterostructure with covalent bond between the CNT and graphene nanoribbons at the two sides[102]. (d) Theoretical density of states (DOS) of the covalent bonded CNT-graphene heterostructure, the DOS of a hydrogenated CNT is plotted in the lower panel as a reference[102].

To form a seamless CNT-graphene heterostructure, a least-square method is utilized to achieve C-C bond-lengths or bond-angles as close as possible to those of the ideal case [103, 104]. Moreover, Euler's theorem is utilized to select the polygons for the contact stitching process [103-108]. Figure 7a shows the possible connections that the eight open bonds of a (4,4) CNT or (8, 0) CNT can form with the underlying graphene sheet[103]. Many theoretical calculations have adopted the same rules to form seamless CNT-graphene heterostructures [71,109]. After identifying the bond contact spots on the graphene surface and the CNT, molecular dynamic simulations are performed to minimize the total binding energy of the heterostructure. For structure relaxation, a full quantum mechanical optimization including force-field relaxation of the nuclei as well as the electrons is necessary. However, such optimization requires prohibitive amount of time and computational resources[110].

Therefore, another approach is employed to achieve force-field convergence using classical molecular dynamics approach, which neglects electron interactions[91, 111, 112]. The advantage of such an approach is drastically reduced computational time, albeit with less accuracy of the final optimized structure.

3.2.1 Electronic Transport Properties

With the optimized heterostructure, one can perform first-principle calculations to obtain electronic properties such as band structure, transmission coefficient, DOS, and conductance. Matsumoto[85] used a tight-binding method to study various (6,6) CNT-graphene heterostructures, including CNT with open tip or capped, and CNT sandwiched between two graphene layers similar to that in Figure 1f. The total energy minimization method is adopted to optimize the geometries using the tight-binding method. Although the (6,6) CNT is metallic, sizable direct bandgaps of 0.27 eV and 0.51 eV were predicted for the open and capped CNT-graphene heterostructures, respectively. An even larger bandgap was predicted for the sandwiched heterostructure. Another interesting structure proposed by Mao[113] also showed a similar effect that the metallic (5,5) CNT was transformed into a semiconductor with a bandgap of 0.2 eV. Strictly speaking, this structure is not a seamless CNT-graphene heterostructure, because the CNT is inserted into the graphene and the two ends of the CNT are connected to the graphene sheets through a hole on each. Nevertheless, a covalent bond is formed between each atom at the graphene hole edge and an atom on the CNT sidewall. This strong coupling results in a bandgap in the metallic (5,5) CNT. In contrast, the original bandgap of 0.65 eV vanishes for a semiconducting (8,0) CNT, because of the induced impurity states by the sp^3-like hybridization between the CNT and the holed graphene. Thus, one may conclude from the above theoretical study that the pristine CNT bandgap can be changed due to the strong covalent bond formed at the CNT-graphene interface.

Since the tight-binding method could not capture the junction-induced band offset between CNT and graphene[85], a first-principle calculation was performed

by Frederico[49] to study the electronic transport properties of the (4,4) and (8,0) CNT-graphene heterostructures. For the metallic (4,4) CNT-graphene heterostructures, two kinds of symmetrical connections containing six heptagonal rings at the interface (No. 3 and No. 9 in Figure 7a) were adopted. The unit cell of the periodic 3D seamless heterostructure shown in Figure 7b was constructed for electronic transport calculations using the non-equilibrium Green's function (NEGF) method, and the current flow is through the CNT-graphene junction and the CNT itself. The calculated transmission coefficient was between 0.01 and 1 and shows a weak dependence on the CNT length in the range of 2.2-4.2 nm, indicating a clear ballistic transport characteristic of the (4,4) metallic CNT-graphene heterostructure. The conductance deduced from the transmission curves also shows a similar weak dependence on CNT length for metallic CNTs as shown in Figure 7c. On the other hand, the conductance shows strong dependence on the contact structure, with the No. 9 contact structure exhibiting a higher transmission and conductance than the No. 3 case. In contrast, the conductance of the semiconducting (8,0) CNT-graphene heterostructure shows a strong dependence on the CNT length and weak dependence on the contact structure. Another interesting point for the (8,0) CNT-graphene heterostructure is that a relatively large conductance is predicted for the heterostructure with a small CNT length of 2 nm (Figure 7c), showing the effect of tunneling. Although the study reveals some interesting electronic transport properties of the CNT-graphene heterostructure, their calculation cannot ascertain the exact contribution of the CNT-graphene junction to the total conductance.

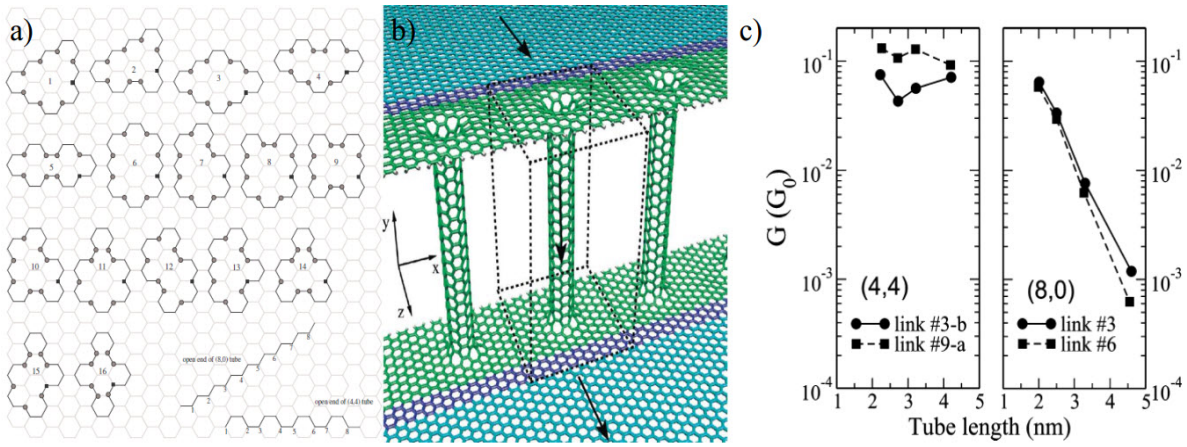

Figure 7. (a) Possible ways to seamlessly connecting (4,4) or (8,0) CNT with graphene [103]. (b) Graphene-CNT-graphene heterostructure used to calculate the transmission coefficient, with the arrows showing the electron transport directions[49]. (c) Deduced conductance of the heterostructure with different CNT type and tube length[49].

To better understand the CNT-graphene contact properties, we have performed calculations on a two-point structure with the NEGF method. To extract the CNT-graphene contact resistance, graphene resistance, and CNT resistance, we calculate the current-voltage (I-V) characteristics of the graphene-CNT-graphene heterostructure shown in Figure 8a. Toward this end, we first compute the resistance of a graphene sheet for different lengths, which turns out to be 6.45 kΩ and independent of length, confirming ballistic transport. This result also serves as a validation of the calculation method. A typical I-V curve for the complete two-point structure is shown in Figure 8b. The total resistance is found to be 91.5 kΩ for the heterostructure with a 2.44 nm long (8,0) CNT. The linear I-V behavior indicates ohmic conduction across the CNT-graphene junction and possibly along the CNT as well. Furthermore, we have also verified the previous study that semiconducting CNTs when contacted with graphene leads to metallic behavior. The DOS and the transmission coefficients of the (8,0) CNT-graphene heterostructure are shown in Figure 8c and 8d, respectively. A finite DOS exists at the Fermi-level (located at 0 eV), representative of the metallic nature of the CNT. The transmission coefficient

shown in Figure 8d also suggests that transmission indeed occurs at the Fermi-level because of the available states.

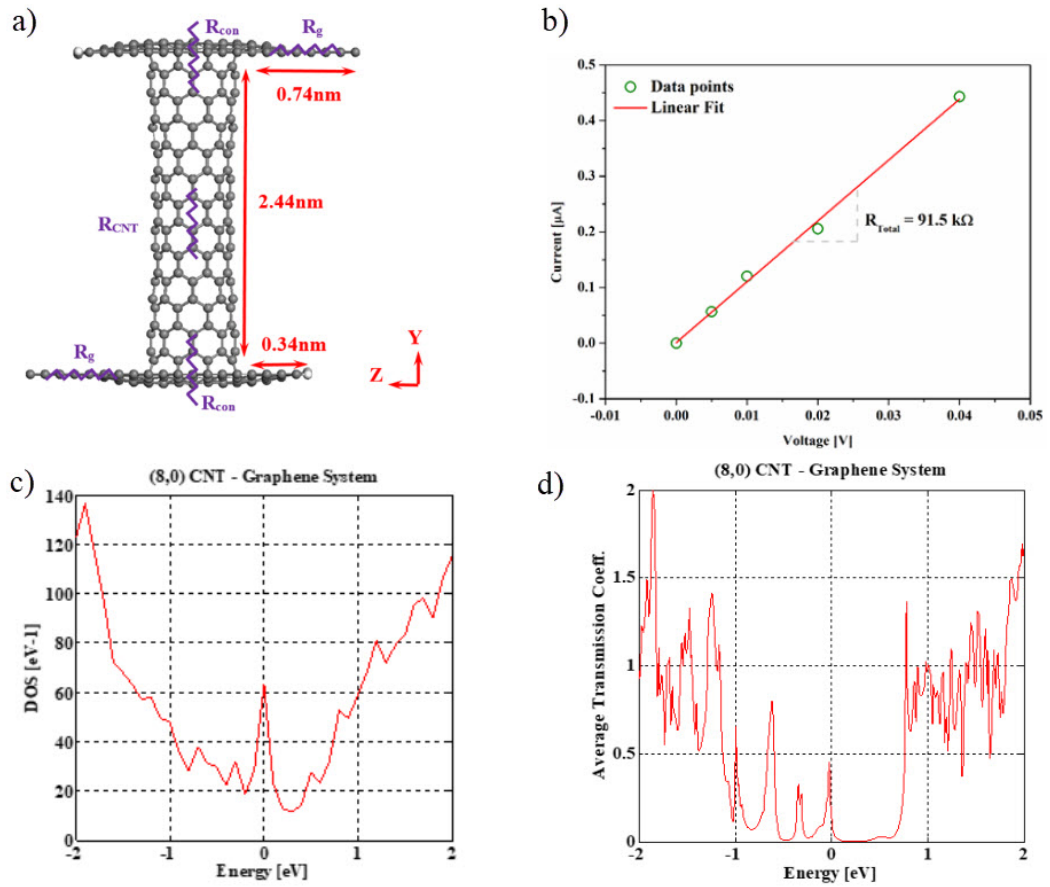

Figure 8. (a) Graphene-CNT-graphene heterostructure used for I-V calculations. (b) I-V curve of the graphene-CNT-graphene heterostructure. (c) DOS and (d) Transmission coefficients of the (8,0) CNT graphene system, showing finite DOS and transmission at Fermi-level (0 eV).

3.2.2 Thermal Transport Properties

Both CNT and graphene possess outstanding intrinsic thermal conductivity, but the high thermal conductivity is only achievable along the CNT length and in-plane directions in graphene. Vertical CNT arrays have been considered as a good thermal interface material (TIM) for its high thermal conductivity along its length[114]. However, the interface between the CNT and the substrate constitutes much of the thermal resistance, which limits the overall performance of the thermal interfacial layer. Recently, many theoretical works have studied the seamless 3D CNT-graphene heterostructure for its superior thermal transport properties [75, 76, 115]. The

heat flow in the 3D seamless CNT-graphene heterostructure was determined to be analogous to current flow [76].

Varshney[76] compared the thermal conductivity k of the heterostructure with an 8-layer graphite and a pure (6, 6) CNT. The in-plane thermal conductivity $k_{//}$ of the heterostructure is inferior to that of an 8-layer graphite, and it increases linearly with the distance between adjacent CNTs in the heterostructure. This can be due to the presence of less scattering sites for a larger CNT-CNT distance. The out-of-plane thermal conductivity $k_{\perp}$ follows a similar trend that a larger CNT length results in a larger $k_{\perp}$. While CNT-CNT distance affects the overall cross-sectional area of the heterostructure, the CNT length determines the phonon scattering length between the two CNT-graphene junctions separated by one vertical CNT. In general, the $k_{//}$ is much higher than the $k_{\perp}$. For example, the $k_{//}$ and $k_{\perp}$ are 9.6 W/m.K and 2.25 W/m.K, respectively, for a heterostructure with a CNT-CNT distance of 9 Å. Thus, the two factors must be optimized to obtain an overall high k in both directions for practical applications.

Chen[75] compared $k_{\perp}$ of a seamless (6,6) CNT-graphene heterostructure with the pristine graphene, and found that the former is at least one order of magnitude larger than the latter. $k_{\perp}$ increases with increasing CNT densities, and it reaches about 100 W/m.K when the density of CNT is about 10%. For efficient cooling of a hot surface, the heterostructure could be immersed into a liquid to speed up heat dissipation[116]. To identify the contribution of the CNT-graphene junction to the total thermal resistance, Shi[117] analyzed the temperature profile throughout the heterostructure, and found that the temperature jump at the junction contributed to most of the total thermal resistance. The calculated covalent CNT-graphene junction resistance of 4.1×10^{-11} m^2K/W ~7.2×10^{-11} m^2K/W is much lower than those of other thermal interface materials. On the other hand, if CNT is weakly connected to the graphene by van der Waals bond, the calculated junction resistance surged up to 4×10^{-8} m^2K/W, clearly suggesting seamless covalent bonding between CNT and

graphene facilitates phonon transport from in-plane direction to out-of-plane direction. A practical application was considered by Bao[118], who studied the CNT-graphene heterostructure for heat dissipation from a silicon substrate. Compared to the CNT-silicon interface, the insertion of a graphene layer between CNT and silicon improved the thermal conductance by more than 40%[118]. Although most of the theoretical study constructed similar seamless CNT-graphene structures as described above, Zhang[115] proposed a novel structure with a transition cone area between the vertical CNT and the parallel graphene so that the contact area could be much larger than the CNT area itself. Compared to the normal CNT-graphene heterostructure, the proposed structure exhibited an improved thermal conductance, which even outperformed the pristine 20 Å-diameter CNT if the cone radius reaches 40Å. These results suggest alternative ways to construct the CNT-graphene heterostructure, which can be experimentally realized[115].

As alluded in section 2, MWCNTs are quite common in grown CNT-graphene heterostructures, yet few theoretical studies on their transport properties exist, partly due to the computation resources requirement to construct and calculate these complex systems. In terms of the MWCNT-MWCNT contact where van der Waals bonds are formed between the carbon atoms at the outer walls, Varshney[119] stressed the importance of effective contact area which is affected by diameter, the number of walls, and the curvature effect in determining the thermal transfer rate across the contact area. However, there is no reported study of the seamless MWCNT-graphene heterostructure to date. With proper structure construction schemes and powerful computation resources, the more complex MWCNT-graphene heterostructure could conceivably reveal new information for comparison with experiment.

Even though the synthesized heterostructures are still quite different from the theoretical model structures, the introduction of the heterostructure is motivated largely by applications requiring better electronic and/or thermal transport

properties and larger surface to volume ratio, which cannot be obtained with only one form of nanocarbon material. As discussed in the next section, there are potential applications that show superior properties of the heterostructure. More studies are needed to relate the measured properties of micro or macroscale heterostructures to theoretical predictions based on a single nanoscale CNT-graphene junction.

4. Potential Applications

Due to the excellent properties of graphene and CNTs, CNT-graphene heterostructures have been proposed as electrodes, catalysts, as well as materials for hydrogen storage and interconnects. In this section, examples are given stressing the advantages of using CNT-graphene heterostructures for such applications.

4.1 Electrodes

For electrodes, a large and efficient conducting area is the key parameter. The large conducting surface of graphene makes it an attractive candidate. However, because of the aggregation of graphene, electrodes composed of graphene alone would not be the optimal choice. Considering the electrical conductivity of CNTs, the combination of vertically aligned CNTs on graphene holds great promise as a superior electrode The CNT-graphene electrode, also called all-carbon electrode, has more effective conducting surface than graphene while retaining its high mechanical flexibility, resulting in larger electron transfer capacity[65]. In addition, the resistance of the CNT-graphene heterostructure is smaller than that of the graphene[72], which can also enhance electronic transmission. Thus, CNT-graphene electrode can be a great candidate for supercapacitors [42, 52, 120]. Using parallel CNT-graphene heterostructure as electrodes[120], a supercapacitor yielded a specific capacitance of 290.4 $F \cdot g^{-1}$. Figure 9a shows the comparison of specific capacitances of CNT, graphene, graphene/CNT composite supercapacitors at different charging

current densities, which indicates the superior performance of the composite supercapacitor. Using vertical CNT-graphene heterostructure, a high-performance supercapacitor has been fabricated with a capacitance of 385 $F \cdot g^{-1}$ at a scan rate of 10 $mV \cdot s^{-1}$ in 6M KOH solution, with high electrochemical stability [52]. Another supercapacitor was reported to exhibit a capacitance of 653.7 $\mu F \cdot cm^{-2}$ at 10 $mV \cdot s^{-1}$, and the capacitance of the heterostructure is higher than that of graphene, as shown in Figure 9b [42]. Besides supercapacitors, the CNT-graphene electrode can also be applied to solar cell. Because of the larger conducting surface, the dye-sensitized solar cell showed a fill factor of 0.7 by using a CNT-graphene heterostructure as the electrode, as shown in Figure 9c [60]. Thus, the enhanced effective surface area and low resistance can create immense potential for CNT-graphene electrode in supercapacitors or solar cells, which are renewable and pollution-free energy storage devices.

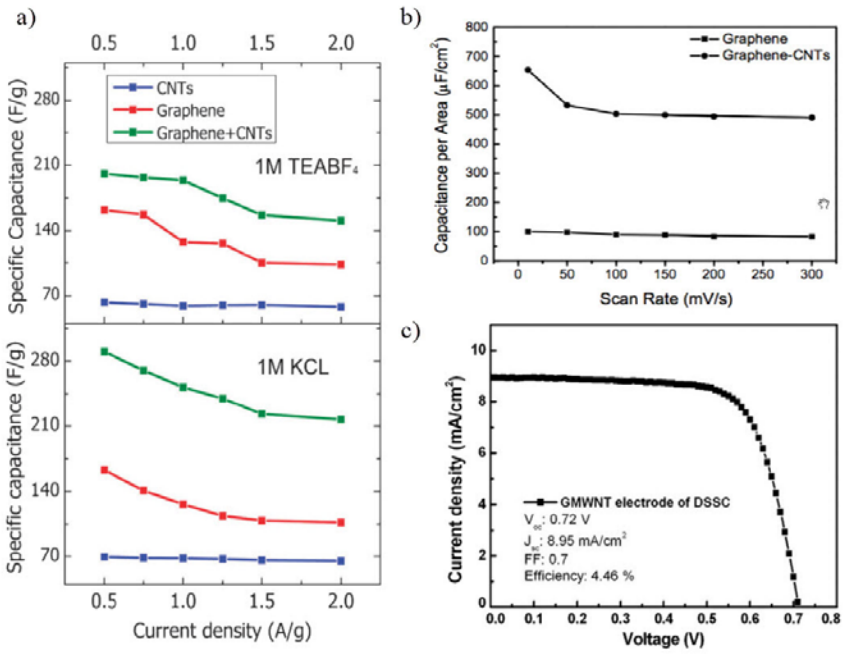

Figure 9. (a) Comparison of specific capacitance of CNT, graphene and parallel CNT-graphene heterostructure supercapacitors at different charging current densities [120]. (b) Capacitance of vertical CNT-graphene heterostructure and graphene at scan rates of 10–300 $mV \cdot s^{-1}$ [42]. (c) Current density vs voltage behavior of dye-sensitized solar cell with a CNT-graphene electrode [60].

4.2 Catalysts

In recent years, CNT-graphene heterostructure has also been studied as potential metal-free catalyst [121-123]. By using the one-step method, SWCNTs and graphene can grow simultaneously on a graphene oxide (GO) substrate. By in situ doping in the growth process, a new N-doped graphene/SWCNT hybrid (NGSH) material can be obtained[121]. Figure 10a shows that N-doped vertical CNT-graphene heterostructure electrode has higher current density than vertical Pt/C electrode [121]. Because SWCNTs have higher surface-to-volume ratio, this NGSH structure possessed a large specific surface area of 812.9 $m^2 \cdot g^{-1}$ and high electrical conductivity of 53.8 $S \cdot cm^{-1}$. It turned out that the hybrid structure was a high-performance and low-cost catalyst for both oxygen reduction reaction and oxygen evolution reaction. Its high oxygen reduction reaction activity was even better than the commercial 20 wt% Pt/C catalysts because of its better durability and low resistance [121]. Apart from N-doped CNT-graphene heterostructure[121,122], Se-doped CNT-graphene heterostructure also showed excellent electrocatalytic activity[123]. Figure 10b and 10c show that the Se-CNTs-graphene heterostructure has the lowest resistance. Thus, using novel doping and growth methods can lead to functionalizing metal-free catalysts using CNT-graphene heterostructures in the future.

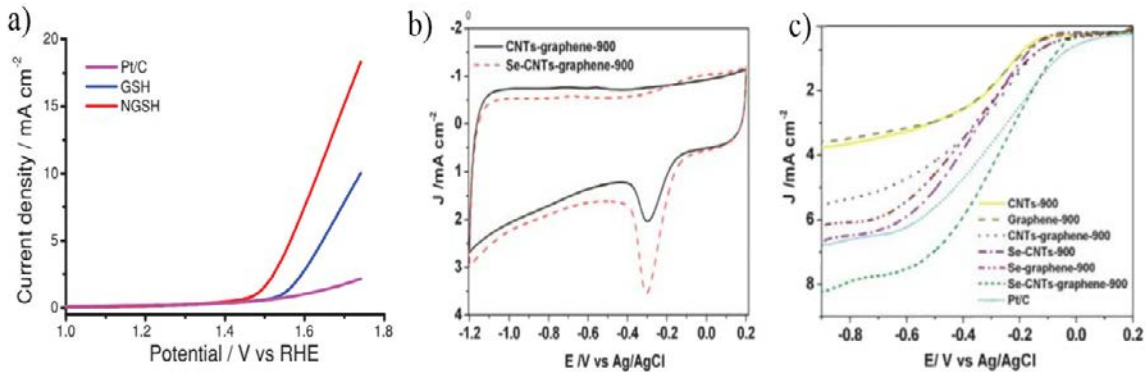

Figure 10. (a) Oxide evolution reduction current density of Pt/C, CNT-graphene and

N-doped CNT-graphene electrodes in 0.1 mol/L KOH solution at 5mV/s[121]. (b) Cyclic voltammetry curves of CNT-graphene heterostructure before and after doping with Se[123]. (c) Linear sweep voltammetry curves for CNT, graphene and CNT-graphene heterostructure before and after doping with Se[123].

4.3 Hydrogen storage

It is known that hydrogen can be an energy source, but its storage capacity is low due to the van der Waals force between hydrogen molecules and the size of the metal container. A vertical CNT-graphene heterostructure can offer an alternative to store hydrogen, as its pore size and surface area can be adjusted by varying the growth process parameters. Theoretical study was conducted and showed that this structure can be effective in increasing storage capacity[71]. When doped with lithium cations, this structure yielded 41 g of H_2/L[71], close to the volumetric requirement of United States Department of Energy for mobile applications, which is 45 g of H_2/L. A simulation of the stacking of the vertical CNT-graphene heterostructure for hydrogen storage is depicted in Figure 11a. Thus, successful fabrication of the stacked CNT-graphene heterostructure can lead to a new hydrogen storage device in the future.

4.4 Interconnects

Continuous downward scaling in chip manufacturing has become a major challenge for on-chip interconnects. Due to electromigration challenges, on-chip Cu interconnect linewidth can no longer be reduced further in current technology nodes. Because of their high current capacity and superior transport properties, graphene[124, 125] and CNTs[33] have become potential candidates to replace Cu interconnects. However, the contact resistance between CNTs and conventional metal is a major challenge in functionalizing CNT vias[33]. Therefore, an all-carbon interconnect network consisting of vertical CNTs on horizontal graphene could mitigate the contact resistance challenge. Although the contact between CNTs and

graphene can be refined to yield low resistance and variability, the contact resistivity can only be low as ~10^{-5} Ω·cm^2 [66], which is still high. Further, to facilitate the proper chip operation, CNTs must be grown on graphene at temperatures compatible to chip manufacturing, such as 550℃[48], 510℃[67]and 400℃[68]. A schematic diagram for using CNTs and graphene as interconnects is shown in Figure 11b. The results in Figures 11c and 11d suggest that conduction path does exist in a 3D CNT-graphene heterostructure. However, contact resistance still remains the critical challenge in its implementation [91].

5. Summary and Conclusions

Structures, growth, properties, and potential applications of various CNT-graphene heterostructures have been reviewed, with emphasis on targeting a specific performance enhancement for a given application. For a parallel CNT-graphene heterostructure, where the CNT axis is parallel to the graphene plane, the main advantages are enhanced mechanical strength and increase in electrical conduction paths, providing a suitable candidate material for flexible electronics and all-carbon transistors. For a vertical CNT-graphene heterostructure, a covalently bonded seamless CNT-graphene junction has been proposed to reduce the electrical and/or thermal contact resistance due to its superior electron and phonon transport properties. Although the structures studied theoretically are still limited to small-diameter single-walled CNT-graphene heterojunctions, significant new findings have been obtained. One example is the opening of a bandgap for a metallic CNT, while a semiconducting CNT can be transformed into metallic under certain heterostructure configurations.

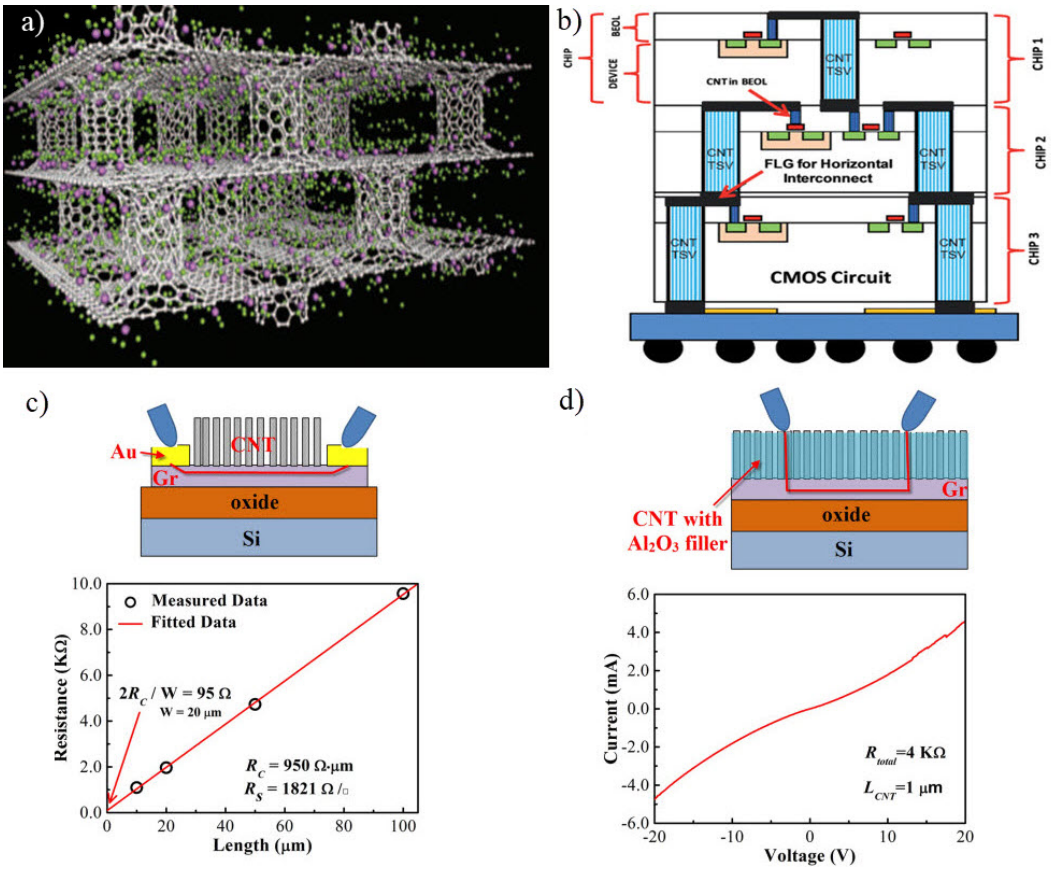

Figure 11. (a) Simulated Li-doped vertical CNT-graphene heterostructure [71]. Green for hydrogen molecules and purple for lithium atoms. (b) Schematic of vertical CNT-graphene heterostructures as interconnects in CMOS circuit[48]. (c) A schematic of the electrical measurement and resistance versus graphene length behavior after CNT growth[91]. (d) Schematic of the electrical measurement and I–V characteristics of the vertical CNT-graphene heterostructure[91].

It is well known that controlled synthesis of semiconducting CNTs for transistor applications is still a challenge, while in the case of CNT-graphene heterostructures for interconnect applications, semiconducting CNT is not needed. We suggest that future theoretical study focuses on the transformation of semiconducting CNT into metallic to support experimental efforts in controlled synthesis. To bridge the gap between theory and experiment, more theoretical studies on MWCNT-graphene heterostructures should be initiated.

Most of the CNT-graphene heterostructures have been synthesized by CVD

methods, which are usually adapted from the CNT growth recipes with careful control of catalyst deposition and catalyst-substrate interactions. Several works have reported TEM analyses of the CNT-graphene interface in attempting to reveal the C-C bonding across the interface [48, 60, 67, 70, 88, 126]. Thus far, the experimental findings, in conjunction with atomistic models used in theoretical calculations, are still a long way from being conclusive on the interfacial atomic arrangements. Therefore, novel techniques are needed to reveal detailed interfacial information. For example, the ratio of sp^2/sp^3 bonding can be extracted from the measured density of states, if an atomically clean CNT-graphene junction can be prepared for advanced TEM and STM analyses. The latter poses a great challenge in experimental study of this heterostructure, while overcoming such challenge would yield enormous gain in understanding the heterostructure.

Currently, the applications of CNT-graphene heterostructures in electronics, thermal interface materials, and electrochemistry have mainly focused on macroscale properties, such as electrical and thermal resistances. In the near future, with more detailed theoretical investigations and controlled syntheses of high-quality CNT-graphene heterostructures, we hope that their superior electron and phonon transport properties can be harnessed to build devices in the nanoscale, and applications such as nano-transistors, advanced-node on-chip interconnects, and thermal interface materials can be realized.

Acknowledgements: This study is supported by National Natural Science Foundation of China (Grant 11804102), the Science and Technology Program of Guangzhou (201804010393, 201807010072), Fundamental Research Funds for the Central Universities and the Key Laboratories Program (614280104051709). Changjian Zhou would like to acknowledge the support from Guangdong Pearl River Youth Talent Recruitment Program.

[1] Kroto, H. W., J. R. Heath, S. C. O'Brien, R. F. Curl and R. E. Smalley 1985 C60: Buckminsterfullerene, Nature. **318** 162-163

[2] Georgakilas, V., J. A. Perman, J. Tucek and R. Zboril 2015 Broad Family of Carbon Nanoallotropes: Classification, Chemistry, and Applications of Fullerenes, Carbon Dots, Nanotubes, Graphene, Nanodiamonds, and Combined Superstructures, Chemical Reviews. **115** 4744-4822

[3] Povie, G., Y. Segawa, T. Nishihara, Y. Miyauchi and K. Itami 2017 Synthesis of a carbon nanobelt, Science. **356** 172-175

[4] De Volder, M. F. L., S. H. Tawfick, R. H. Baughman and A. J. Hart 2013 Carbon Nanotubes: Present and Future Commercial Applications, Science. **339** 535-539

[5] Ferrari, A. C., F. Bonaccorso, V. Fal'ko, K. S. Novoselov, S. Roche, P. Bøggild, S. Borini, F. H. L. Koppens, V. Palermo, N. Pugno, J. A. Garrido, R. Sordan, A. Bianco, L. Ballerini, M. Prato, E. Lidorikis, J. Kivioja, C. Marinelli, T. Ryhänen, A. Morpurgo, J. N. Coleman, V. Nicolosi, L. Colombo, A. Fert, M. Garcia-Hernandez, A. Bachtold, G. F. Schneider, F. Guinea, C. Dekker, M. Barbone, Z. Sun, C. Galiotis, A. N. Grigorenko, G. Konstantatos, A. Kis, M. Katsnelson, L. Vandersypen, A. Loiseau, V. Morandi, D. Neumaier, E. Treossi, V. Pellegrini, M. Polini, A. Tredicucci, G. M. Williams, B. Hee Hong, J.-H. Ahn, J. Min Kim, H. Zirath, B. J. van Wees, H. van der Zant, L. Occhipinti, A. Di Matteo, I. A. Kinloch, T. Seyller, E. Quesnel, X. Feng, K. Teo, N. Rupesinghe, P. Hakonen, S. R. T. Neil, Q. Tannock, T. Löfwander and J. Kinaret 2015 Science and technology roadmap for graphene, related two-dimensional crystals, and hybrid systems, Nanoscale. **7** 4598-4810

[6] Zhang, Y., T.-T. Tang, C. Girit, Z. Hao, M. C. Martin, A. Zettl, M. F. Crommie, Y. R. Shen and F. Wang 2009 Direct observation of a widely tunable bandgap in bilayer graphene, Nature. **459** 820-823

[7] Yu, Y.-J., Y. Zhao, S. Ryu, L. E. Brus, K. S. Kim and P. Kim 2009 Tuning the Graphene Work Function by Electric Field Effect, Nano Letters. **9** 3430-3434

[8] Chen, C.-W., M.-H. Lee and S. J. Clark 2004 Band gap modification of single-walled carbon nanotube and boron nitride nanotube under a transverse electric field, Nanotechnology. **15** 1837-1843

[9] Chiu, Y. H., Y. H. Lai, J. H. Ho, D. S. Chuu and M. F. Lin 2008 Electronic structure of a two-dimensional graphene monolayer in a spatially modulated magnetic field: Peierls tight-binding model, Physical Review B. **77** 045407

[10] Jarillo-Herrero, P., J. Kong, H. S. J. van der Zant, C. Dekker, L. P. Kouwenhoven and S. De Franceschi 2005 Electronic Transport Spectroscopy of Carbon Nanotubes in a Magnetic Field, Physical Review Letters. **94** 156802

[11] Si, C., Z. Sun and F. Liu 2016 Strain engineering of graphene: a review, Nanoscale. **8** 3207-3217

[12] Naumis, G. G., S. Barraza-Lopez, M. Oliva-Leyva and H. Terrones 2017 Electronic and optical properties of strained graphene and other strained 2D materials: a review, Reports on Progress in Physics. **80** 096501

[13] Ni, G.-X., H.-Z. Yang, W. Ji, S.-J. Baeck, C.-T. Toh, J.-H. Ahn, V. M. Pereira and B. Özyilmaz 2014 Tuning Optical Conductivity of Large-Scale CVD Graphene by Strain Engineering, Advanced materials. **26** 1081-1086

[14] Wang, C., K. Takei, T. Takahashi and A. Javey 2013 Carbon nanotube electronics – moving forward, Chem. Soc. Rev. **42** 2592-2609

[15] Avouris, P. 2010 Graphene: Electronic and Photonic Properties and Devices, Nano Letters. **10** 4285-4294

[16] Lu, C.-H., H.-H. Yang, C.-L. Zhu, X. Chen and G.-N. Chen 2009 A Graphene Platform for Sensing Biomolecules, Angewandte Chemie International Edition. **48** 4785-4787

[17] Tang, X., S. Bansaruntip, N. Nakayama, E. Yenilmez, Y.-l. Chang and Q. Wang 2006 Carbon Nanotube DNA Sensor and Sensing Mechanism, Nano Letters. **6** 1632-1636

[18] Navas, H., M. Picher, A. Andrieux-Ledier, F. Fossard, T. Michel, A. Kozawa, T. Maruyama, E. Anglaret,

A. Loiseau and V. Jourdain 2017 Unveiling the Evolutions of Nanotube Diameter Distribution during the Growth of Single-Walled Carbon Nanotubes, ACS nano. **11** 3081-3088
[19] Mattevi, C., H. Kim and M. Chhowalla 2011 A review of chemical vapour deposition of graphene on copper, J. Mater. Chem. **21** 3324-3334
[20] Hafizi, R., J. Tersoff and V. Perebeinos 2017 Band Structure and Contact Resistance of Carbon Nanotubes Deformed by a Metal Contact, Physical Review Letters. **119** 207701
[21] Jiang, Y., P. Wang and L. Lin 2011 Characterizations of contact and sheet resistances of vertically aligned carbon nanotube forests with intrinsic bottom contacts, Nanotechnology. **22** 365704
[22] Lim, S. C., J. H. Jang, D. J. Bae, G. H. Han, S. Lee, I.-S. Yeo and Y. H. Lee 2009 Contact resistance between metal and carbon nanotube interconnects: Effect of work function and wettability, Applied Physics Letters. **95** 264103
[23] Léonard, F. and A. A. Talin 2011 Electrical contacts to one- and two-dimensional nanomaterials, Nature Nanotechnology. **6** 773-783
[24] Wilhite, P., A. A. Vyas, J. Tan, J. Tan, T. Yamada, P. Wang, J. Park and C. Y. Yang 2014 Metal–nanocarbon contacts, Semiconductor Science and Technology. **29** 054006
[25] Matsuda, Y., W.-Q. Deng and W. A. Goddard 2010 Contact Resistance for "End-Contacted" Metal−Graphene and Metal−Nanotube Interfaces from Quantum Mechanics, The Journal of Physical Chemistry C. **114** 17845-17850
[26] Nagashio, K., T. Nishimura, K. Kita and A. Toriumi Metal/graphene contact as a performance Killer of ultra-high mobility graphene analysis of intrinsic mobility and contact resistance, *2009 IEEE International Electron Devices Meeting (IEDM)*. 1-4
[27] Jang, K.-T., S.-Y. Lee, S.-K. Na, S.-K. Lee, J.-M. Baek, W.-K. You, O.-H. Park, R.-H. Kim, H.-S. Oh and Y.-C. Joo 2018 Electromigration Characteristics and Morphological Evolution of Cu Interconnects on CVD Co and Ru Liners for 10-nm Class VLSI Technology, IEEE Electron Device Letters. **39** 1050-1053
[28] Ward, J. W., J. Nichols, T. B. Stachowiak, Q. Ngo and E. J. Egerton 2012 Reduction of CNT Interconnect Resistance for the Replacement of Cu for Future Technology Nodes, IEEE Transactions on Nanotechnology. **11** 56-62
[29] Kreup, F., A. P. Graham, M. Liebau, G. S. Duesberg, R. Seidel and E. Unger Carbon nanotubes for interconnect applications, *IEDM Technical Digest. IEEE International Electron Devices Meeting, 2004.* 683-686
[30] Awano, Y., S. Sato, M. Nihei, T. Sakai, Y. Ohno and T. Mizutani 2010 Carbon Nanotubes for VLSI: Interconnect and Transistor Applications, Proceedings of the IEEE. **98** 2015-2031
[31] Graham, A. P., G. S. Duesberg, W. Hoenlein, F. Kreupl, M. Liebau, R. Martin, B. Rajasekharan, W. Pamler, R. Seidel, W. Steinhoegl and E. Unger 2005 How do carbon nanotubes fit into the semiconductor roadmap?, Applied Physics A. **80** 1141-1151
[32] Vyas, A. A., C. Zhou, P. Wilhite, P. Wang and C. Y. Yang 2016 Electrical properties of carbon nanotube via interconnects for 30nm linewidth and beyond, Microelectronics Reliability. **61** 35-42
[33] Zhou, C., A. A. Vyas, P. Wilhite, P. Wang, M. Chan and C. Y. Yang 2015 Resistance Determination for Sub-100-nm Carbon Nanotube Vias, IEEE Electron Device Letters. **36** 71-73
[34] Wu, W., S. Krishnan, T. Yamada, X. Sun, P. Wilhite, R. Wu, K. Li and C. Y. Yang 2009 Contact resistance in carbon nanostructure via interconnects, Applied Physics Letters. **94** 163113
[35] Veen, M. H. v. d., Y. Barbarin, B. Vereecke, M. Sugiura, Y. Kashiwagi, D. J. Cott, C. Huyghebaert and Z. Tökei Electrical improvement of CNT contacts with Cu damascene top metallization, *2013 IEEE International Interconnect Technology Conference - IITC*. 1-3
[36] Zhu, Y., L. Li, C. Zhang, G. Casillas, Z. Sun, Z. Yan, G. Ruan, Z. Peng, A. R. Raji, C. Kittrell, R. H. Hauge

and J. M. Tour 2012 A seamless three-dimensional carbon nanotube graphene hybrid material, Nat Commun. **3** 1225
[37] El-Kady, M. F., V. Strong, S. Dubin and R. B. Kaner 2012 Laser Scribing of High-Performance and Flexible Graphene-Based Electrochemical Capacitors, Science. **335** 1326-1330
[38] Yen, M.-Y., M.-C. Hsiao, S.-H. Liao, P.-I. Liu, H.-M. Tsai, C.-C. M. Ma, N.-W. Pu and M.-D. Ger 2011 Preparation of graphene/multi-walled carbon nanotube hybrid and its use as photoanodes of dye-sensitized solar cells, Carbon. **49** 3597-3606
[39] Kaempgen, M., C. K. Chan, J. Ma, Y. Cui and G. Gruner 2009 Printable Thin Film Supercapacitors Using Single-Walled Carbon Nanotubes, Nano Letters. **9** 1872-1876
[40] Li, D., M. B. Müller, S. Gilje, R. B. Kaner and G. G. Wallace 2008 Processable aqueous dispersions of graphene nanosheets, Nature Nanotechnology. **3** 101-105
[41] Saleh, N. B., L. D. Pfefferle and M. Elimelech 2008 Aggregation Kinetics of Multiwalled Carbon Nanotubes in Aquatic Systems: Measurements and Environmental Implications, Environmental Science & Technology. **42** 7963-7969
[42] Kim, Y. S., K. Kumar, F. T. Fisher and E. H. Yang 2012 Out-of-plane growth of CNTs on graphene for supercapacitor applications, Nanotechnology. **23** 015301
[43] You, B., L. Wang, L. Yao and J. Yang 2013 Three dimensional N-doped graphene–CNT networks for supercapacitor, Chemical Communications. **49** 5016
[44] Wang, J., F. Ma, W. Liang and M. Sun 2017 Electrical properties and applications of graphene, hexagonal boron nitride (h-BN), and graphene/h-BN heterostructures, Materials Today Physics. **2** 6-34
[45] Wang, J., X. Mu, X. Wang, N. Wang, F. Ma, W. Liang and M. Sun 2018 The thermal and thermoelectric properties of in-plane C-BN hybrid structures and graphene/h-BN van der Waals heterostructures, Materials Today Physics. **5** 29-57
[46] Wang, J., F. Ma, W. Liang, R. Wang and M. Sun 2017 Optical, photonic and optoelectronic properties of graphene, h-BN and their hybrid materials, Nanophotonics. **6** 943-976
[47] Wang, J., X. Xu, X. Mu, F. Ma and M. Sun 2017 Magnetics and spintronics on two-dimensional composite materials of graphene/hexagonal boron nitride, Materials Today Physics. **3** 93-117
[48] Ghosh, K., N. Ranjan, Y. K. Verma and C. S. Tan 2016 Graphene–CNT hetero-structure for next generation interconnects, RSC Advances. **6** 53054-53061
[49] Novaes, F. D., R. Rurali and P. Ordejón 2010 Electronic Transport between Graphene Layers Covalently Connected by Carbon Nanotubes, ACS Nano. **4** 7596-7602
[50] Lee, D. H., J. E. Kim, T. H. Han, J. W. Hwang, S. Jeon, S. Y. Choi, S. H. Hong, W. J. Lee, R. S. Ruoff and S. O. Kim 2010 Versatile carbon hybrid films composed of vertical carbon nanotubes grown on mechanically compliant graphene films, Advanced materials. **22** 1247-1252
[51] Qin, H., Y. Sun, J. Z. Liu and Y. Liu 2017 Enhanced in-plane mechanical properties of nanoporous graphene-carbon nanotube network, Journal of Applied Physics. **121** 215104
[52] Fan, Z., J. Yan, L. Zhi, Q. Zhang, T. Wei, J. Feng, M. Zhang, W. Qian and F. Wei 2010 A Three-Dimensional Carbon Nanotube/Graphene Sandwich and Its Application as Electrode in Supercapacitors, Advanced Materials. **22** 3723-3728
[53] Tessonnier, J.-P. and D. S. Su 2011 Recent Progress on the Growth Mechanism of Carbon Nanotubes: A Review, ChemSusChem. **4** 824-847
[54] Bae, S., H. Kim, Y. Lee, X. Xu, J.-S. Park, Y. Zheng, J. Balakrishnan, T. Lei, H. Ri Kim, Y. I. Song, Y.-J. Kim, K. S. Kim, B. Özyilmaz, J.-H. Ahn, B. H. Hong and S. Iijima 2010 Roll-to-roll production of 30-inch graphene films for transparent electrodes, Nature Nanotechnology. **5** 574
[55] Wu, S., E. Shi, Y. Yang, W. Xu, X. Li and A. Cao 2015 Direct fabrication of carbon nanotube-graphene

hybrid films by a blown bubble method, Nano Research. **8** 1746-1754
[56] Shi, E., H. Li, L. Yang, J. Hou, Y. Li, L. Li, A. Cao and Y. Fang 2015 Carbon nanotube network embroidered graphene films for monolithic all-carbon electronics, Advanced materials. **27** 682-688
[57] Hunley, D. P., S. L. Johnson, J. K. Stieha, A. Sundararajan, A. T. Meacham, I. N. Ivanov and D. R. Strachan 2011 Crystallographically Aligned Carbon Nanotubes Grown on Few-Layer Graphene Films, ACS nano. **5** 6403-6409
[58] Yan, Z., Z. Peng, G. Casillas, J. Lin, C. Xiang, H. Zhou, Y. Yang, G. Ruan, A.-R. O. Raji, E. L. G. Samuel, R. H. Hauge, M. J. Yacaman and J. M. Tour 2014 Rebar Graphene, ACS nano. **8** 5061-5068
[59] Maarouf, A. A., A. Kasry, B. Chandra and G. J. Martyna 2016 A graphene–carbon nanotube hybrid material for photovoltaic applications, Carbon. **102** 74-80
[60] Choi, H., H. Kim, S. Hwang, M. Kang, D.-W. Jung and M. Jeon 2011 Electrochemical electrodes of graphene-based carbon nanotubes grown by chemical vapor deposition, Scripta Materialia. **64** 601-604
[61] Li, X., G. Zhu and Z. Xu 2012 Nitrogen-doped carbon nanotube arrays grown on graphene substrate, Thin Solid Films. **520** 1959-1964
[62] Nguyen, D. D., N. H. Tai, S. Y. Chen and Y. L. Chueh 2012 Controlled growth of carbon nanotube-graphene hybrid materials for flexible and transparent conductors and electron field emitters, Nanoscale. **4** 632-638
[63] Kumar, K., Y.-S. Kim, X. Li, J. Ding, F. T. Fisher and E.-H. Yang 2013 Chemical Vapor Deposition of Carbon Nanotubes on Monolayer Graphene Substrates: Reduced Etching via Suppressed Catalytic Hydrogenation Using C2H4, Chemistry of Materials. **25** 3874-3879
[64] Rao, R., G. Chen, L. M. Arava, K. Kalaga, M. Ishigami, T. F. Heinz, P. M. Ajayan and A. R. Harutyunyan 2013 Graphene as an atomically thin interface for growth of vertically aligned carbon nanotubes, Scientific reports. **3** 1891
[65] Ryu, J. H., G. J. Lee, W. S. Kim, H. E. Lim, M. Mativenga, K. C. Park and H. K. Park 2014 All-Carbon Electrode Consisting of Carbon Nanotubes on Graphite Foil for Flexible Electrochemical Applications, Materials. **7** 1975-1983
[66] Ramos, R., A. Fournier, M. Fayolle, J. Dijon, C. P. Murray and J. McKenna Nanocarbon interconnects combining vertical CNT interconnects and horizontal graphene lines, *2016 IEEE International Interconnect Technology Conference / Advanced Metallization Conference (IITC/AMC)*. 48-50
[67] Kondo, D., S. Sato and Y. Awano 2008 Self-organization of Novel Carbon Composite Structure: Graphene Multi-Layers Combined Perpendicularly with Aligned Carbon Nanotubes, Applied Physics Express. **1** 074003
[68] Jousseaume, V., J. Cuzzocrea, N. Bernier and V. T. Renard 2011 Few graphene layers/carbon nanotube composites grown at complementary-metal-oxide-semiconductor compatible temperature, Applied Physics Letters. **98** 123103
[69] Choi, J. W., S. K. Youn and H. G. Park 2013 Carbon Micronymphaea: Graphene on Vertically Aligned Carbon Nanotubes, Journal of Nanomaterials. **2013** 1-7
[70] Salvatierra, R. V., D. Zakhidov, J. Sha, N. D. Kim, S. K. Lee, A. O. Raji, N. Zhao and J. M. Tour 2017 Graphene Carbon Nanotube Carpets Grown Using Binary Catalysts for High-Performance Lithium-Ion Capacitors, ACS nano. **11** 2724-2733
[71] Dimitrakakis, G. K., E. Tylianakis and G. E. Froudakis 2008 Pillared Graphene: A New 3-D Network Nanostructure for Enhanced Hydrogen Storage, Nano Letters. **8** 3166-3170
[72] Gao, M., Z. L. Huang, B. Zeng, T. S. Pan, Y. Zhang, H. B. Peng and Y. Lin 2015 Carbon nanotube-graphene junctions studied by impedance spectra, Applied Physics Letters. **106** 051601
[73] Fan, Z., J. Yan, L. Zhi, Q. Zhang, T. Wei, J. Feng, M. Zhang, W. Qian and F. Wei 2010 A three-

dimensional carbon nanotube/graphene sandwich and its application as electrode in supercapacitors, Advanced materials. **22** 3723-3728
[74] Du, F., D. Yu, L. Dai, S. Ganguli, V. Varshney and A. K. Roy 2011 Preparation of Tunable 3D Pillared Carbon Nanotube–Graphene Networks for High-Performance Capacitance, Chemistry of Materials. **23** 4810-4816
[75] Chen, J., J. H. Walther and P. Koumoutsakos 2015 Covalently Bonded Graphene-Carbon Nanotube Hybrid for High-Performance Thermal Interfaces, Advanced Functional Materials. **25** 7539-7545
[76] Varshney, V., S. S. Patnaik, A. K. Roy, G. Froudakis and B. L. Farmer 2010 Modeling of Thermal Transport in Pillared-Graphene Architectures, ACS Nano. **4** 1153-1161
[77] Jiang, J., Y. Li, C. Gao, N. D. Kim, X. Fan, G. Wang, Z. Peng, R. H. Hauge and J. M. Tour 2016 Growing Carbon Nanotubes from Both Sides of Graphene, ACS applied materials & interfaces. **8** 7356-7362
[78] Dupuis, A. 2005 The catalyst in the CCVD of carbon nanotubes—a review, Progress in Materials Science. **50** 929-961
[79] Muñoz, R. and C. Gómez-Aleixandre 2013 Review of CVD Synthesis of Graphene, Chemical Vapor Deposition. **19** 297-322
[80] Zhang, Y., L. Zhang and C. Zhou 2013 Review of Chemical Vapor Deposition of Graphene and Related Applications, Accounts of Chemical Research. **46** 2329-2339
[81] Van Chuc, N., C. T. Thanh, N. Van Tu, V. T. Q. Phuong, P. V. Thang and N. T. Thanh Tam 2015 A Simple Approach to the Fabrication of Graphene-Carbon Nanotube Hybrid Films on Copper Substrate by Chemical Vapor Deposition, Journal of Materials Science & Technology. **31** 479-483
[82] Shi, E., H. Li, L. Yang, J. Hou, Y. Li, L. Li, A. Cao and Y. Fang 2015 Carbon Nanotube Network Embroidered Graphene Films for Monolithic All-Carbon Electronics, Advanced Materials. **27** 682-688
[83] Lin, X., P. Liu, Y. Wei, Q. Li, J. Wang, Y. Wu, C. Feng, L. Zhang, S. Fan and K. Jiang 2013 Development of an ultra-thin film comprised of a graphene membrane and carbon nanotube vein support, Nature Communications. **4** 2920
[84] Engels, S., P. Weber, B. Terres, J. Dauber, C. Meyer, C. Volk, S. Trellenkamp, U. Wichmann and C. Stampfer 2013 Fabrication of coupled graphene-nanotube quantum devices, Nanotechnology. **24** 035204
[85] Matsumoto, T. and S. Saito 2002 Geometric and Electronic Structure of New Carbon-Network Materials: Nanotube Array on Graphite Sheet, Journal of the Physical Society of Japan. **71** 2765-2770
[86] Dang, V. T., D. D. Nguyen, T. T. Cao, P. H. Le, D. L. Tran, N. M. Phan and V. C. Nguyen 2016 Recent trends in preparation and application of carbon nanotube–graphene hybrid thin films, Advances in Natural Sciences: Nanoscience and Nanotechnology. **7** 033002
[87] Ping, L., P. X. Hou, C. Liu, J. Li, Y. Zhao, F. Zhang, C. Ma, K. Tai, H. Cong and H. M. Cheng 2017 Surface-restrained growth of vertically aligned carbon nanotube arrays with excellent thermal transport performance, Nanoscale. **9** 8213-8219
[88] Rout, C. S., A. Kumar, T. S. Fisher, U. K. Gautam, Y. Bando and D. Golberg 2012 Synthesis of chemically bonded CNT–graphene heterostructure arrays, RSC Advances. **2** 8250
[89] Yan, Z., L. Ma, Y. Zhu, I. Lahiri, M. G. Hahm, Z. Liu, S. Yang, C. Xiang, W. Lu, Z. Peng, Z. Sun, C. Kittrell, J. Lou, W. Choi, P. M. Ajayan and J. M. Tour 2013 Three-Dimensional Metal–Graphene–Nanotube Multifunctional Hybrid Materials, ACS nano. **7** 58-64
[90] Jyothirmayee Aravind, S. S., V. Eswaraiah and S. Ramaprabhu 2011 Facile synthesis of one dimensional graphene wrapped carbon nanotube composites by chemical vapour deposition, Journal of Materials Chemistry. **21** 15179
[91] Zhou, C., R. Senegor, Z. Baron, Y. Chen, S. Raju, A. A. Vyas, M. Chan, Y. Chai and C. Y. Yang 2017

Synthesis and interface characterization of CNTs on graphene, Nanotechnology. **28** 054007
[92] Zhao, M.-Q., X.-F. Liu, Q. Zhang, G.-L. Tian, J.-Q. Huang, W. Zhu and F. Wei 2012 Graphene/Single-Walled Carbon Nanotube Hybrids: One-Step Catalytic Growth and Applications for High-Rate Li–S Batteries, ACS nano. **6** 10759-10769
[93] Tian, G. L., M. Q. Zhao, D. Yu, X. Y. Kong, J. Q. Huang, Q. Zhang and F. Wei 2014 Nitrogen-doped graphene/carbon nanotube hybrids: in situ formation on bifunctional catalysts and their superior electrocatalytic activity for oxygen evolution/reduction reaction, Small. **10** 2251-2259
[94] Xue, Y., Y. Ding, J. Niu, Z. Xia, A. Roy, H. Chen, J. Qu, Z. L. Wang and L. Dai 2015 Rationally designed graphene-nanotube 3D architectures with a seamless nodal junction for efficient energy conversion and storage, Sci Adv. **1** 2375-2548
[95] Ho, Y. H., Y. H. Chiu, J. M. Lu and M. F. Lin 2010 Low-energy electronic structures of nanotube–graphene hybrid carbon systems, Physica E: Low-dimensional Systems and Nanostructures. **42** 744-747
[96] Cook, B. G., W. R. French and K. Varga 2012 Electron transport properties of carbon nanotube–graphene contacts, Applied Physics Letters. **101** 153501
[97] Robert, P. T. and R. Danneau 2014 Charge distribution of metallic single walled carbon nanotube–graphene junctions, New Journal of Physics. **16** 013019
[98] Chai, Y., A. Hazeghi, K. Takei, H.-Y. Chen, P. C. H. Chan, A. Javey and H. S. P. Wong 2012 Low-Resistance Electrical Contact to Carbon Nanotubes With Graphitic Interfacial Layer, IEEE Transactions on Electron Devices. **59** 12-19
[99] Gangavarapu, P. R. Y., P. C. Lokesh, K. N. Bhat and A. K. Naik 2017 Graphene Electrodes as Barrier-Free Contacts for Carbon Nanotube Field-Effect Transistors, IEEE Transactions on Electron Devices. **64** 4335-4339
[100] Ivanovskaya, V. V., A. Zobelli, P. Wagner, M. I. Heggie, P. R. Briddon, M. J. Rayson and C. P. Ewels 2011 Low-Energy Termination of Graphene Edges via the Formation of Narrow Nanotubes, Physical Review Letters. **107** 065502
[101] Akhukov, M. A., S. Yuan, A. Fasolino and M. I. Katsnelson 2012 Electronic, magnetic and transport properties of graphene ribbons terminated by nanotubes, New Journal of Physics. **14** 123012
[102] Artyukh, A. A., L. A. Chernozatonskii and P. B. Sorokin 2010 Mechanical and electronic properties of carbon nanotube-graphene compounds, physica status solidi (b). **247** 2927-2930
[103] Baowan, D., B. J. Cox and J. M. Hill 2007 Two least squares analyses of bond lengths and bond angles for the joining of carbon nanotubes to graphenes, Carbon. **45** 2972-2980
[104] Baowan, D., B. J. Cox, N. Thamwattana and J. M. Hill 2009 Two Minimisation Approximations for Joining Carbon Nanostructures, IUTAM Symposium on Modelling Nanomaterials and Nanosystems. 109-121
[105] Kroto, H. W. 1987 The stability of the fullerenes Cn, with n = 24, 28, 32, 36, 50, 60 and 70, Nature. **329** 529-531
[106] Terrones, H. and A. L. Mackay 1992 The Geometry of Hypothetical Curved Graphite Structures, Carbon. **30** 1251-1260
[107] Terrones, H. and M. Terrones 2003 Curved nanostructured materials, New Journal of Physics. **5** 126
[108] Ebbesen, T. W. and T. Takada 1995 Topological and SP3 defect structures in nanotubes, Carbon. **33** 973-978
[109] Yang, N., D. Yang, L. Chen, D. Liu, M. Cai and X. Fan 2017 A First-Principle Theoretical Study of Mechanical and Electronic Properties in Graphene Single-Walled Carbon Nanotube Junctions, Materials. **10** 1300

[110] Taylor, J., H. Guo and J. Wang 2001 Ab initiomodeling of quantum transport properties of molecular electronic devices, Physical Review B. **63** 245407
[111] Soler, J. M., E. Artacho, J. D. Gale, A. García, J. Junquera, P. Ordejón and D. Sánchez-Portal 2002 The SIESTA method forab initioorder-Nmaterials simulation, Journal of Physics: Condensed Matter. **14** 2745-2779
[112] Hanwell, M. D., D. E. Curtis, D. C. Lonie, T. Vandermeersch, E. Zurek and G. R. Hutchison 2012 Avogadro: an advanced semantic chemical editor, visualization, and analysis platform, Journal of Cheminformatics. **4** 17
[113] Mao, Y. and J. Zhong 2009 The computational design of junctions by carbon nanotube insertion into a graphene matrix, New Journal of Physics. **11** 093002
[114] Huang, H., C. H. Liu, Y. Wu and S. Fan 2005 Aligned Carbon Nanotube Composite Films for Thermal Management, Advanced Materials. **17** 1652-1656
[115] Zhang, Z., A. Kutana, A. Roy and B. I. Yakobson 2017 Nanochimneys: Topology and Thermal Conductance of 3D Nanotube–Graphene Cone Junctions, The Journal of Physical Chemistry C. **121** 1257-1262
[116] Chen, J., J. H. Walther and P. Koumoutsakos 2016 Ultrafast cooling by covalently bonded graphene-carbon nanotube hybrid immersed in water, Nanotechnology. **27** 465705
[117] Shi, J., Y. Dong, T. Fisher and X. Ruan 2015 Thermal transport across carbon nanotube-graphene covalent and van der Waals junctions, Journal of Applied Physics. **118** 044302
[118] Bao, H., C. Shao, S. Luo and M. Hu 2014 Enhancement of interfacial thermal transport by carbon nanotube-graphene junction, Journal of Applied Physics. **115** 053524
[119] Varshney, V., J. Lee, D. Li, J. S. Brown, B. L. Farmer, A. A. Voevodin and A. K. Roy 2017 Understanding thermal conductance across multi-wall carbon nanotube contacts: Role of nanotube curvature, Carbon. **114** 15-22
[120] Cheng, Q., J. Tang, J. Ma, H. Zhang, N. Shinya and L. C. Qin 2011 Graphene and carbon nanotube composite electrodes for supercapacitors with ultra-high energy density, Phys Chem Chem Phys. **13** 17615-17624
[121] Tian, G.-L., M.-Q. Zhao, D. Yu, X.-Y. Kong, J.-Q. Huang, Q. Zhang and F. Wei 2014 Nitrogen-Doped Graphene/Carbon Nanotube Hybrids: In Situ Formation on Bifunctional Catalysts and Their Superior Electrocatalytic Activity for Oxygen Evolution/Reduction Reaction, Small. **10** 2251-2259
[122] Chen, P., T.-Y. Xiao, Y. Qian, S.-S. Li and S.-H. Yu 2013 A Nitrogen-Doped Graphene/Carbon Nanotube Nanocomposite with Synergistically Enhanced Electrochemical Activity, Advanced materials. **25** 3192-3196
[123] Jin, Z., H. Nie, Z. Yang, J. Zhang, Z. Liu, X. Xu and S. Huang 2012 Metal-free selenium doped carbon nanotube/graphene networks as a synergistically improved cathode catalyst for oxygen reduction reaction, Nanoscale. **4** 6455
[124] Xiangyu, C., L. Kyeong-Jae, D. Akinwande, G. F. Close, S. Yasuda, B. Paul, S. Fujita, K. Jing and H. P. Wong High-speed graphene interconnects monolithically integrated with CMOS ring oscillators operating at 1.3GHz, *2009 IEEE International Electron Devices Meeting (IEDM)*. 1-4
[125] Lee, K., A. P. Chandrakasan and J. Kong 2011 Breakdown Current Density of CVD-Grown Multilayer Graphene Interconnects, IEEE Electron Device Letters. **32** 557-559
[126] Lin, C.-Y., Z. Zhao, J. Niu and Z. Xia 2016 Synthesis, properties and applications of 3D carbon nanotube–graphene junctions, Journal of Physics D: Applied Physics. **49** 443001